Positional cloning of *heart and soul* reveals multiple roles for PKCλ in zebrafish organogenesis

Sally Horne-Badovinac*, Dan Lin†‡, Steve Waldron*, Monica Schwarz*, Geraldine Mbamalu‡, Tony Pawson‡, Yuh-Nung Jan§, Didier Y.R. Stainier* and Salim Abdelilah-Seyfried§

Background: The Par-3/Par-6/aPKC complex is a key regulator of cell polarity in a number of systems. In *Drosophila*, this complex acts at the zonula adherens (adherens junctions) to establish epithelial polarity and helps to orient the mitotic spindle during asymmetric neuroblast divisions. In MDCKII cells, this complex localizes to the zonula occludens (tight junctions) and appears to regulate epithelial polarity. However, the in vivo role of this complex during vertebrate embryogenesis is not known, due to the lack of relevant mutations.

Results: We have positionally cloned the zebrafish *heart and soul* (*has*) mutation, which affects the morphogenesis of several embryonic tissues, and show that it encodes atypical protein kinase C lambda (aPKCλ). We find that loss of aPKCλ affects the formation and maintenance of the zonula adherens in the polarized epithelia of the retina, neural tube, and digestive tract, leading to novel phenotypes, such as the formation of multiple lumens in the developing intestine. In addition, *has* mutants display defects in gut looping and endodermal organ morphogenesis that appear to be independent of the defects in epithelial polarity. Finally, we show that loss of aPKCλ leads to defects in spindle orientation during progenitor cell divisions in the neural retina.

Conclusions: Our results show that aPKCλ is required for the formation and maintenance of the zonula adherens during early epithelial development in vertebrates and demonstrate a previously undescribed yet critical role for this protein in organ morphogenesis. Furthermore, our studies identify the first genetic locus regulating the orientation of cell division in vertebrates.

Addresses: *Departments of Biochemistry and Biophysics, Programs in Developmental Biology, Genetics and Human Genetics, University of California-San Francisco, San Francisco, California 94143, USA. †Program in Molecular Biology and Cancer, Samuel Lunenfeld Research Institute, Mount Sinai Hospital, 600 University Avenue, Toronto, Ontario M5G 1X5, Canada. ‡Department of Molecular and Medical Genetics, University of Toronto, Toronto, Ontario M5S 1A8, Canada. §Departments of Physiology and Biochemistry and Biophysics, Howard Hughes Medical Institute, University of California-San Francisco, San Francisco, California 94143, USA.

Correspondence: Didier Y. R. Stainier
E-mail: didier_stainier@biochem.ucsf.edu

Received: **29 June 2001**
Revised: **6 August 2001**
Accepted: **21 August 2001**

Published: **2 October 2001**

Current Biology 2001, 11:1492–1502

0960-9822/01/$ – see front matter
© 2001 Elsevier Science Ltd. All rights reserved.

Background

The formation, maintenance, and movement of epithelial sheets are critical processes during development. Mature epithelial cells have a polarized configuration with separate apical and basolateral membrane domains. These domains have distinct complements of lipids and proteins that are separated by a large junctional complex at the apical side of the lateral membrane. In vertebrates, this apical junctional complex consists of the zonula adherens and the zonula occludens. The zonula adherens is comprised of cadherin/catenin-based adherens junctions, which provide cell-cell adhesion and facilitate apical constriction of cells [1]. The zonula occludens is located just apical to the zonula adherens and consists of tight junctions. These provide a regulated barrier to paracellular diffusion and prevent the mixing of lipids and proteins between the apical and basolateral membrane compartments [2].

In recent years, a highly conserved protein complex has been identified that regulates cell polarity in a wide range of cell types and organisms. The core of this complex consists of the PDZ-containing proteins, Par-3 and Par-6, and an atypical protein kinase C (aPKC). The role of these proteins in the formation of polarized epithelia is best understood from work in *Drosophila*. Bazooka (*Drosophila* Par-3) [3, 4], DmPar-6 [5], and DaPKC [6] localize to the apicolateral membrane in a number of embryonic epithelia. Immunohistochemical analysis has shown that this complex partially overlaps with and extends just apical to Armadillo (β-catenin) localization at the zonula adherens. Loss of function of any one of these genes in *Drosophila* results in a number of epithelial defects, including loss of apical adherens junctions and changes in cell shape. Furthermore, these mutations also result in a high incidence of abnormal spindle orientation during asymmetric neuroblast divisions [4–6], due to mislocalization of the Inscuteable protein.

Less is understood about the role of the Par-3/Par-6/aPKC

Figure 1

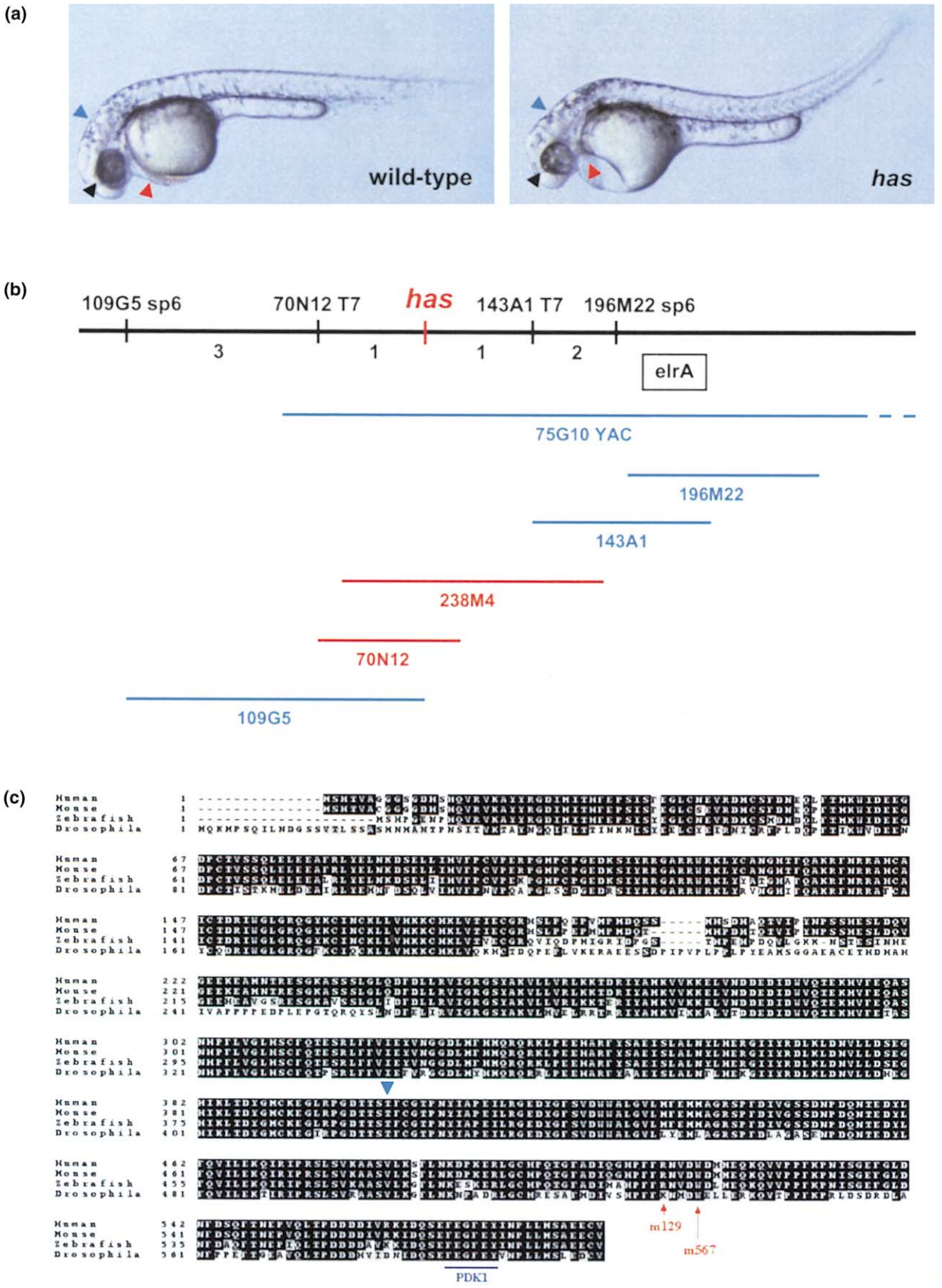
(a)
wild-type
has
(b)
109G5 sp6
70N12 T7
has
143A1 T7
196M22 sp6
3
1
1
2
elrA
75G10 YAC
196M22
143A1
238M4
70N12
109G5
(c)
Human
Mouse
Zebrafish
Drosophila
m129
m567
PDK1

complex in vertebrate epithelia. In MDCK II cells, Par-3 (ASIP), Par-6, and the two highly related vertebrate aPKCs, λ and ζ, colocalize with the tight junction protein, ZO-1, indicating that this complex localizes to the zonula occludens in mature, polarized epithelia [7, 8]. This conclusion is further supported by immunogold electron microscopy, which places Par-3 at the tight junction in the rat intestinal epithelium [7]. Further studies have shown that a dominant-negative form of aPKCλ can disrupt the localization of tight junction proteins, including Claudin and Occludin, when MDCK II cells are depolarized and then repolarized using a calcium switch [8]. aPKCλ and Par-3 have also been observed to colocalize with ZO-1 at adherens junctions in NIH 3T3 cells [7], suggesting that these proteins may localize to other cell junctions in the absence of tight junctions.

In order to gain a firm understanding of the role of this complex in the formation and maintenance of polarized epithelia in vertebrates, loss-of-function mutations need to be identified and analyzed. Large-scale screens for embryonic lethal mutations in zebrafish have identified several mutations that affect epithelial integrity in various organs [9, 10]. One of these mutations is *heart and soul* (*has*), which exhibits defects in heart tube assembly, a disrupted retinal pigmented epithelium (RPE), defects in the neural retina (heretofore referred to as the retina), failure of the brain ventricles to inflate, and abnormal body curvature (Figure 1a) [11–14].

Here, we extend the phenotypic characterization of *has* mutant embryos and report the positional cloning of the *has* gene. *has* encodes an aPKC, most closely related to the λ/ι class of atypical PKCs (referred to as aPKCλ in the remainder of the text). We find that *has* mutants display epithelial defects within the organs of the digestive tract, as well as the eye and neural tube. We show that, during early stages of organogenesis, when epithelial phenotypes first manifest, *has* appears to regulate the clustering and maintenance of apical adherens junctions. We further show that loss of aPKCλ activity leads to defects in spindle orientation during progenitor cell divisions in the retina. *has* represents the first loss-of-function mutation affecting the Par-3/Par-6/aPKC complex in a vertebrate organism and constitutes an important tool for the study of cell polarity, epithelial formation, and organ morphogenesis in vertebrates.

Results

Positional cloning of *has*

We initially mapped the *has* mutation to LG2 by half-tetrad analysis [15], through linkage to the centromeric marker Z4300. Fine mapping on 2940 meioses placed *has* 0.2 cM proximal to *elrA*. We then assembled a contiguous stretch of genomic DNA across the *has* region and, through further fine mapping, localized *has* to two overlapping PACs, 70N12 and 238M4 (Figure 1b). To identify individual genes within this region, we radiolabeled each PAC insert and probed a normalized cDNA library prepared from 24-hours postfertilization (hpf) embryos. Of the 31 positive clones chosen for analysis, 9 mapped to one or both of the PACs by PCR analysis. Sequencing revealed that the nine clones corresponded to three different genes. Two of these genes mapped exclusively to the 238M4 PAC and showed no obvious homology to other genes in the database. The third gene mapped to both the 70N12 and 238M4 PACs and showed high homology to *aPKC*λ.

has encodes aPKCλ

To test whether the *has* phenotype was due to a mutation in *aPKC*λ, we compared cDNA sequences from the wild-type and mutant alleles. This analysis revealed that both alleles encode truncated proteins. The *m129* allele contains a C → T base change at position 1519 that creates a premature stop codon, removing 73 amino acids from the C terminus of the protein. Likewise, a G → A mutation at position 1532 in the *m567* allele results in a premature stop codon that truncates the protein by 69 amino acids (Figure 1c). The striking proximity and similarity of these two lesions corresponds well with the observation that these two alleles are phenotypically indistinguishable.

Although the catalytic domain of aPKCλ is intact in these alleles, we wished to determine whether the kinase activity of the truncated proteins was affected. To test this,

Positional cloning reveals that *has* encodes aPKCλ. **(a)** Comparison of wild-type and *has* mutant embryos at 33 hpf. At this stage, *has* mutants show defects in heart tube assembly (red arrowhead), a patchy RPE (black arrowhead), failure of the brain ventricles to inflate (blue arrowhead), and abnormal body curvature. **(b)** Positional cloning of the *has* gene. PCR primers to the *elrA* gene were used to initiate a chromosome walk, and a contiguous stretch of genomic DNA was assembled across the *has* region using YAC and PAC clones. The numbers between each genetic marker represent the number of recombinational breakpoints between the markers examined. Markers proximal to *has* were tested on 2569 meioses, and markers distal to *has* were tested on 2940 meioses. The 70N12 and 238M4 PACs were subsequently used to screen cDNA filters, and both PACs contain the *aPKC*λ gene. **(c)** Sequence alignment of aPKCλ from human, mouse, and zebrafish and DaPKC from *Drosophila*. Dark shading indicates conserved residues, and light shading marks similar residues. has^{m129} and has^{m567} encode truncated proteins; the positions of the premature stop codons are marked with red arrows. *m129* is R → stop, and *m567* is W → stop. The conserved PDK1 docking site is underlined in blue, and the conserved threonine, which is phosphorylated by PDK1, is marked with a blue arrowhead. *aPKC*λ is expressed broadly and in a dynamic fashion during embryogenesis (see the Supplementary material).

Figure 2

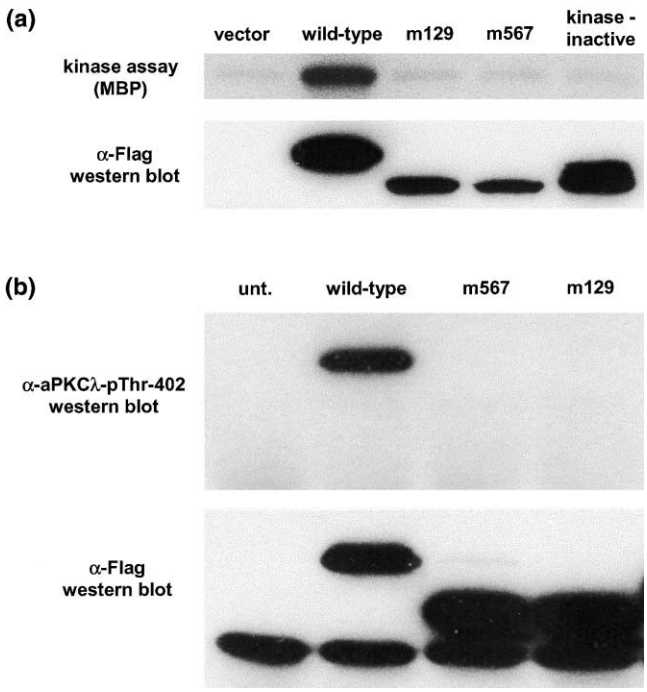

The *m129* and *m567* truncations render murine aPKCλ kinase inactive. **(a)** A kinase assay to examine the effect of the *m129* and *m567* truncations on aPKCλ activity. Site-directed mutagenesis was used to recreate the *m129* and *m567* mutations in mouse *aPKC*λ in order to compare the kinase activity of the resulting truncated proteins with wild-type and kinase-inactive (K273E) versions of the enzyme. Constructs were Flag tagged and transfected into 293T cells. Proteins were immunoprecipitated from cell lysates, and relative protein levels were examined on a Western blot using an antibody against the Flag epitope (lower panel). In the kinase-inactive lane of the Western blot, the band appears as a triplet, likely due to the use of two alternate methionine start sites in this construct. Kinase activity was assessed in vitro using myelin basic protein (MBP) as a substrate. The activity of the *m129* and *m567* truncations is indistinguishable from the kinase-inactive version of the protein (upper panel). **(b)** A Western blot to examine the phosphorylation state of Thr-402 in the T loop of aPKCλ. Transfections and immunoprecipitations were carried out as described above. The upper panel shows that only the wild-type protein is phosphorylated on Thr-402. In the lower panel, the upper bands in lanes 2–4 demonstrate that protein levels from the immunoprecipitation are roughly equivalent, while the lower band that is present in all lanes is the immunoglobulin heavy chain from the FLAG antibody. unt., untransfected.

we introduced the corresponding *m129* and *m567* mutations in the murine aPKCλ cDNA and assayed catalytic activity using an in vitro kinase reaction. Specifically, exogenously expressed Flag-tagged aPKCλ proteins were immunoprecipitated and incubated with myelin basic protein (MBP) as a substrate. Figure 2a shows that, in contrast to the wild-type Flag aPKCλ, both the *m129* and *m567* truncated proteins exhibit little to no kinase activity toward MBP. In fact, the kinase activity of the mutant proteins is indistinguishable from a form of the protein rendered kinase inactive by a K273E mutation. The kinase assay gave similar results using Enolase as a substrate (data not shown).

One explanation for the loss of catalytic activity in the corresponding *m129* and *m567* mutations in murine aPKCλ is that both truncated proteins lack a highly conserved 3-phosphoinositide-dependent protein kinase-1 (PDK1) binding site that is located in the C terminus of aPKCλ [16]. The presence of this critical docking site is required for an activating phosphorylation of aPKCs on a conserved threonine residue in the T loop of the kinase domain by PDK1 [17]. To test this hypothesis, we employed an antibody that specifically recognizes the phosphorylated state of Thr-402 within the T loop of the protein. A comparison of the exogenously expressed wild-type protein with the truncated mutant gene products on a Western blot revealed that only the wild-type protein was phosphorylated on Thr-402 by endogenous PDK1 in transiently transfected 293T cells (Figure 2b). Together, these data strongly suggest that the gene products of the *m129* and *m567* alleles are catalytically inactive.

To gain final confirmation that *has* corresponds to *aPKC*λ, we showed that microinjection of *aPKC*λ mRNA into zebrafish embryos at the 1- to 4-cell stage was sufficient to rescue the *has* mutant phenotype (see the Supplementary material available with this article online). In addition, we found that injection of a morpholino antisense oligonucleotide [18] against *aPKC*λ produced a phenotype that is highly similar, although somewhat more severe, to that seen in *has* mutants (see the Supplementary material). Together with the genetic linkage, molecular lesions, and biochemical evidence, these data strongly argue that *has* encodes aPKCλ.

Dysmorphology of the digestive tract organs in *has* mutant embryos

In light of the role aPKCs play in the formation of polarized epithelia in *Drosophila* and MDCKII cells, we examined the formation of various epithelial tissues in *has* mutants. In particular, we focused our studies on the digestive tract and retina, as these tissues allowed high-resolution analysis at both the cellular and organ level.

Examination of the developing digestive tract revealed striking morphogenetic defects in *has* mutants. By 30 hpf in wild-type, the gut tube primordium has looped to the left [19]. In *has* mutants, the gut primordium fails to loop and remains in the midline (data not shown). At 48 hpf in wild-type, the intestine (I) remains on the left, and now the primordia of three organs are present. The liver (L) is on the left, the swimbladder (S) is dorsal and lies roughly in the midline, and the pancreas (P) projects to the right (Figure 3a). In *has* mutants, the swimbladder is small, and the liver and pancreas adopt symmetrical positions (Figure 3b).

Figure 3

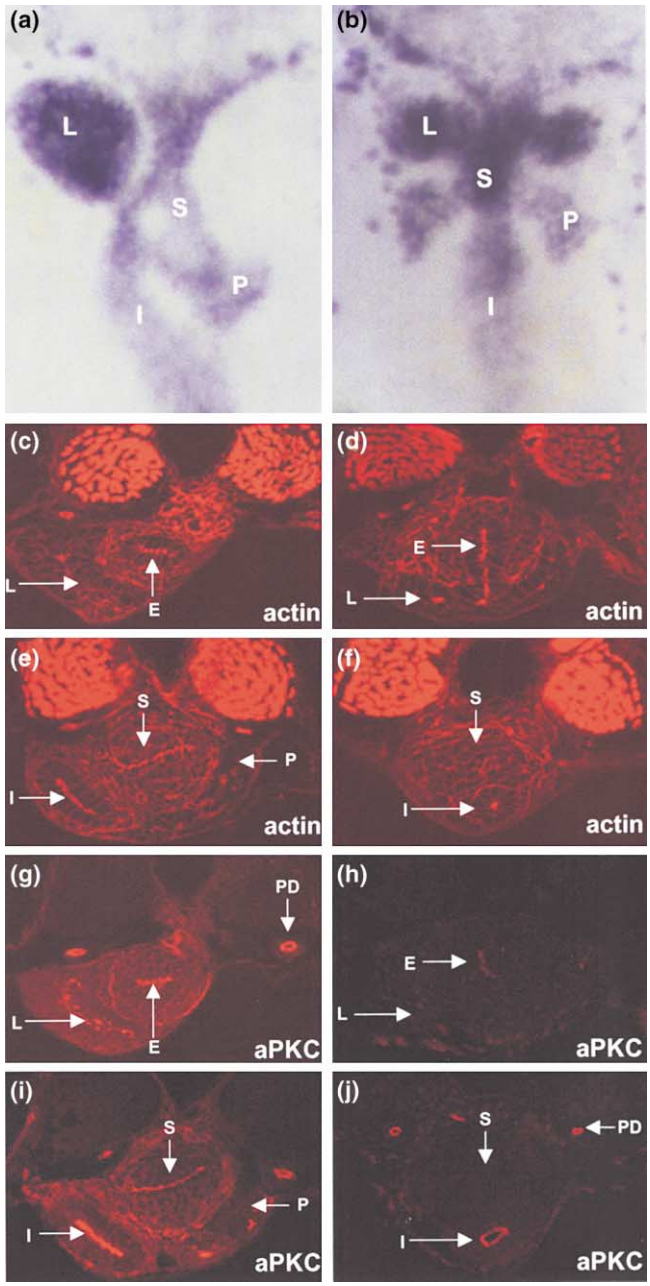

Morphological defects and subcellular localization of aPKCs in the digestive organs. **(a,b)** Dorsal views, anterior is oriented toward the top. A whole-mount in situ hybridization with *foxA3*. (a) In wild-type embryos, the gut tube primordium loops to the left, placing the liver (L) on the left, the swimbladder (S) in the midline, and the pancreas (P) on the right. (b) In *has* mutants, the gut tube primordium and a small swimbladder are in the midline, and the liver and pancreas adopt symmetrical positions. **(c–f)** Transverse sections stained with rhodamine-phalloidin, dorsal is oriented toward the top. (c) In wild-type embryos, the esophagus (E) lies near the midline, and the liver is on the left. (d) In *has* mutants, the liver is ventral to the esophagus. Note the apical actin belt in the esophageal endoderm, which is oriented horizontally in wild-type and vertically in mutants (c,d). (e) There is strong apical actin staining in the endodermal linings of the swimbladder and the intestine (I) in wild-type embryos. (f) In *has* mutants, the endodermal lining of the swimbladder does not form a polarized epithelium, and the intestine is in the midline. **(g–j)** Transverse sections stained with an antibody that recognizes the C terminus of both aPKCλ and aPKCζ. Because the *m129* and *m567* alleles of *has* lack the C terminus, they are not recognized by this antibody. In wild-type, there is apical staining in the (g) polarized epithelia of the esophagus and pronephric ducts (PD) as well as in the (i) endodermal lining of the swimbladder and intestine. Patchy staining is observed in the (g) liver and (i) pancreas, and there is diffuse staining throughout the (g) liver. (g,i) Finally, aPKCλ is found throughout the mesodermal mesenchyme surrounding the digestive organs. *has* mutants lack much of this staining, indicating that aPKCλ is the predominant aPKC in these regions. (j) However, there is immunoreactivity in the pronephric ducts and intestine. (h) There is also weak staining in the esophagus. This staining observed in *has* mutants may be due to the presence of aPKCζ or residual full-length aPKCλ. All embryos are 48 hpf.

To better visualize cell and organ morphologies, we stained transverse sections through these organs with rhodamine-phalloidin. In addition to labeling the cortical actin in each cell, phalloidin also marks the apical actin belt at the zonula adherens, providing general information about epithelial polarity within these organs. Figure 3c shows a cross-section through a wild-type embryo at 48 hpf. The endodermal portion of the esophagus (E) is near the midline, surrounded by a thick layer of mesodermal mesenchyme, and the liver projects to the left of the esophagus. By contrast, the liver in *has* mutants is a single, elongated structure ventral to the esophagus (Figure 3d).

In a more posterior section through wild-type (Figure 3e), the swimbladder appears as a large, round structure near the midline. The bulk of this organ primordium is composed of mesodermal mesenchyme, but there is also a thin endodermal lining, which forms a polarized epithelium (note the strong apical localization of actin). In *has* mutants, the endodermal lining of the swimbladder is morphologically indistinguishable from the surrounding mesenchyme, as it fails to form a polarized epithelium (Figure 3f). Altogether, these data indicate that aPKCλ plays a critical role in digestive organ morphogenesis as well as in the formation of a polarized epithelium in the swimbladder.

Localization of aPKC isoforms within the digestive organs

To help elucidate the role of aPKCλ during endodermal organ morphogenesis, we examined its subcellular distribution in these tissues. The antibody we used recognizes both vertebrate aPKC proteins, λ and ζ, but since it was generated against a C-terminal epitope, it does not recognize the truncated proteins encoded by has^{m129} and has^{m567}. By comparing wild-type and mutant embryos, the staining domains of aPKCλ and aPKCζ can be distinguished: staining observed in *has* mutants must be due to aPKCζ and/or residual levels of full-length aPKCλ (see the Supplemen-

tary material), while staining present exclusively in wild-type must correspond to aPKCλ.

We find that, within the digestive tract endoderm, aPKCs show strong apical localization in the polarized epithelia of the swimbladder (Figure 3i), esophagus (Figure 3g), and intestine (Figure 3i). aPKCλ appears to be the only aPKC expressed in the endodermal lining of the swimbladder, as this staining is not present in *has* mutants (Figure 3j). The exclusive expression of aPKCλ in this tissue likely explains the severe polarity phenotype observed in the swimbladder in *has* mutants. In the case of the esophagus, apical staining is present but reduced in *has* mutants, suggesting that both λ and ζ are expressed in this tissue (Figure 3h). aPKCζ appears to be a large component of the apical staining in the intestine (compare Figures 3i and 3j). However, subtle polarity defects in the intestinal epithelium, discussed below, point to a role for aPKCλ in this tissue as well. Finally, we find patchy staining in the liver (Figure 3g) and pancreas (Figure 3i), which may correspond to epithelial tubules in these organs. aPKCλ appears to be the only aPKC expressed in these structures.

In addition to aPKC immunoreactivity within endodermal epithelia, there is also staining throughout the digestive tract mesoderm. This staining is most apparent in the mesenchyme surrounding the esophagus (Figure 3g) and in the mesodermal component of the swimbladder (Figure 3i). This immunoreactivity appears to be exclusive to aPKCλ, as it is missing in *has* mutants (Figure 3h,j).

aPKCλ directs the apical clustering of adherens junctions during intestinal lumen formation

While assessing digestive organ morphology in *has* mutants, we uncovered a particularly striking phenotype in the intestinal epithelium. Cross-sections through the intestinal bulb revealed that this structure can have regions with two or even three lumens (Figure 4g). On first inspection, the apicobasal polarity of the epithelial cells appears normal, as most cells surrounding the lumens have a columnar shape with strong apical localization of actin (Figure 4g), aPKCξ, and ZO-1 (data not shown).

To address how these multiple lumens arise, we used rhodamine-phalloidin to follow the development of cell shape and polarity during gut tube formation. In wild-type zebrafish, endodermal cells migrate to the midline and initially form a multicellular rod with no visible lumen. With time, these cells rearrange in space, polarize, and produce a lumen in the center. Because phalloidin strongly labels the actin associated with adherens junctions, we were able to follow the clustering and apical targeting of these structures during lumen formation. We observed that small foci of adherens junctions form locally between a few cells at a time (Figure 4a). These foci appear to move toward the center of the rod and merge with one another until there is a single medial cluster of adherens junctions (Figure 4b). At this time, the cells display apicobasal polarity, but the apical domain appears to be very small. Finally, a lumen forms within this central spot (Figure 4c). In *has* mutants, this central clustering of adherens junctions appears to be delayed and generally less efficient than in wild-type (Figure 4e). Multiple lumens result when lumen formation begins before the clusters of adherens junctions have converged to the center of the rod (Figure 4f). These observations suggest that aPKCλ regulates the apical clustering of adherens junctions during the initial polarization of intestinal epithelial cells.

The zonula adherens is not maintained in *has* mutant retinae

Prior to neuronal differentiation and lamination, the retina exists as a single sheet of pseudostratified epithelial cells, with its apical (ventricular) surface facing the RPE and its basal (vitreal) domain apposed to the lens. Immunohistochemistry shows distinct apical localization of aPKC proteins within the wild-type retinal neuroepithelium at 32 hpf (Figure 5a). This staining is slightly apical to and partially overlapping with staining for the junctional protein ZO-1 (Figure 5b). We believe that these two proteins localize to the zonula adherens, as this domain also overlaps with apical actin (data not shown). It appears that aPKCλ is the predominant aPKC expressed in this tissue at this stage, as immunoreactivity is greatly reduced in *has* mutants (Figure 5c). Despite the low level of aPKC protein, apical adherens junctions form in *has* mutants. Localization of ZO-1 (Figure 5c) and junctional actin (data not shown) are both normal, and mutant cells show the same elongated morphology as in wild-type (Figure 6a).

Although apical adherens junctions appear to form normally in *has* mutant retinae, these structures are not maintained. Between 30 and 60 hpf in wild-type embryos, the bulk of the various neuronal and nonneuronal cell types in the retina exit the cell cycle, differentiate, and organize into functional laminae [20, 21]. Throughout this dynamic process, apical adherens junctions are maintained at the ventricular surface of the retina, and aPKCs continue to colocalize at these junctions with ZO-1 and β-catenin (Figure 5d,e). In contrast, apical adherens junctions are progressively lost from *has* mutant retinae during this time period. This phenomenon appears to be most pronounced between 40 hpf, when apical junctions still look relatively normal in *has* mutants, as assessed by phalloidin staining, and 50 hpf, when apical junctions appear to be severely reduced (see the Supplementary material). At 60 hpf, there is nearly a complete lack of ZO-1- and β-catenin-positive junctions at the ventricular surface in *has* mutants (Figure 5f). Finally, at 72 hpf, wild-type retinae have a columnar layer of epithelial cells at the ventricular surface,

Figure 4

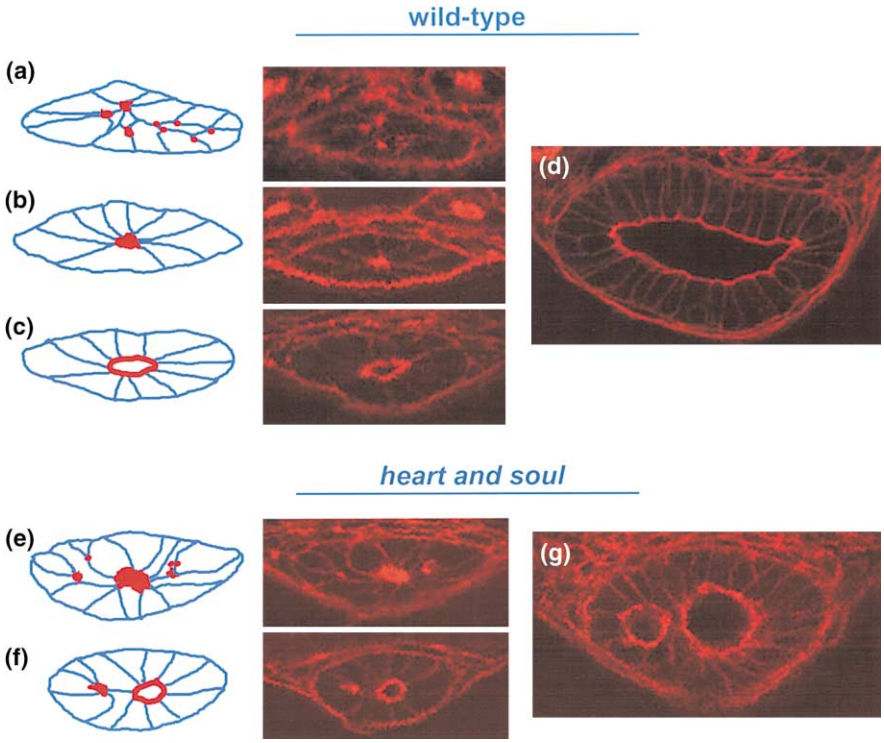

Loss of aPKCλ disrupts the apical clustering of adherens junctions during lumen formation in the intestine. **(a–g)** Photographs show transverse sections through the intestine stained with rhodamine-phalloidin. In the diagrams, red spots correspond to foci of adherens junctions. (a–d) The formation of the intestinal lumen in wild-type embryos. (a,b) At 36 hpf, initially small foci of adherens junctions form locally between a few cells at a time within the rod of gut endoderm (a). (b) These foci appear to move toward the apical side of the cells, merging with one another, until there is a single cluster of adherens junctions in the center of the rod. (c) Around, 42 hpf, a lumen opens within the central spot of adherens junctions. It is unclear how lumen formation occurs, but we speculate that it could be due to expansion of the apical membrane domain. (d) At 60 hpf, the wild-type intestine has a large, single lumen. (e–g) Apical clustering of adherens junctions is disrupted in *has* mutants. (e) At 42 hpf, clustering of adherens junctions occurs in *has* mutants but is far less efficient. (f) At 48 hpf, multiple lumens result when lumens open before all the foci of adherens junctions have made it to the center of the rod. (g) At 60 hpf in *has* mutants, much of the intestine has a single lumen, but occasional regions with multiple lumens are found. In each image, dorsal is oriented toward the top.

whereas mutant retinae only have round, disorganized cells in this location (Figure 5g,h). Apical adherens junctions are also progressively lost from the ventricular surface of the neural tube during the same stages (data not shown). These data indicate that aPKCλ is not only required for the formation of the zonula adherens, as seen in the digestive tract, but for its maintenance as well.

Loss of aPKCλ affects orientation of cell division in the retina

In polarized epithelia, positioning of the mitotic spindle is tightly regulated so that most cell divisions occur within the plane of the epithelium. The situation is more complicated in neuroepithelia such as the retina, however, because spindles occasionally reorient, possibly to allow for asymmetric cell divisions during neurogenesis [22]. Because loss of epithelial polarity is often accompanied by misorientation of the mitotic spindle, we decided to examine cell division patterns in *has* mutant retinae.

During the development of the retina, cell nuclei migrate to the ventricular (apical) surface just prior to division, and the cells release their basal processes, round up, and divide (Figure 6a). In our initial observations of spindle orientation during progenitor cell division, we found that *has* mutants display an increased number of ectopic cell divisions (data not shown). A similar observation has been reported for two other zebrafish mutations [23, 24], and it is believed that these ectopically dividing cells may lack all apicobasal polarity. For our subsequent analysis, we only scored cells dividing at the ventricular surface, because their apical migration indicates that these cells demonstrate at least some aspects of normal apicobasal polarity.

We analyzed the orientation of progenitor cell divisions throughout the proliferative phase in the retina and found that the majority of mitotic spindles (≥90% of total) are oriented parallel to the ventricular surface (Table 1). This observation is consistent with other studies of neuroepithelia in several vertebrate species [25–27]. During these divisions, aPKCs localize to the apical side of progenitor cells and appear to segregate symmetrically into both daughter cells (Figure 6b,d). Only a small fraction of divisions have spindles that are oriented at an angle perpendicular to the ventricular surface. In contrast, *has* mutants show an increased number of cell divisions with abnormal spindle orientations (≥45° out of the horizontal plane) (Figure 6c,e; Table 1), and the relative incidence of reoriented spindles increases significantly between 32 and 50 hpf. At 40 hpf, when apical junctions still appear fairly normal (see the Supplementary material), 18.2% of all cell

Figure 5

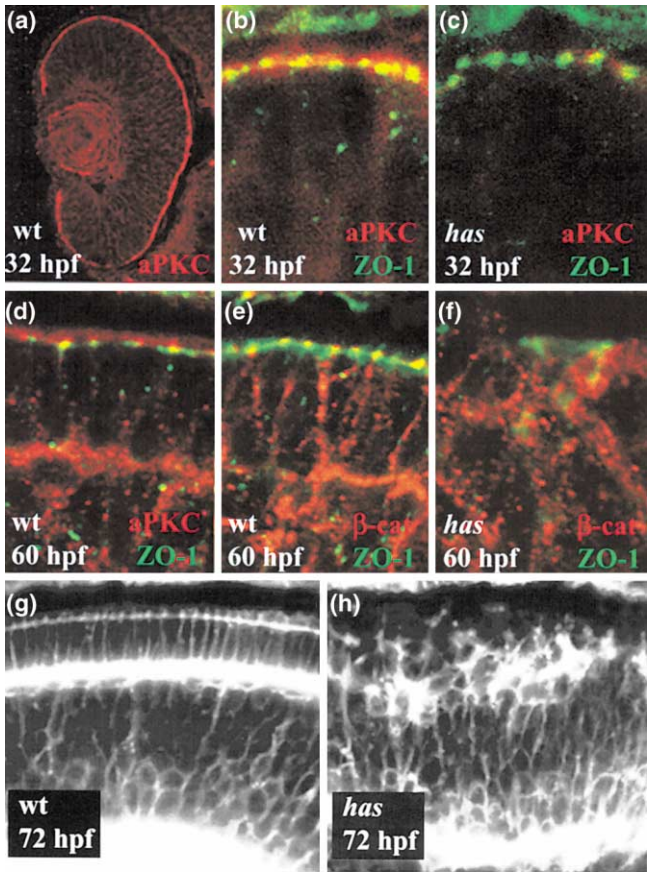

The zonula adherens is not maintained in *has* mutant retinae. **(a–c)** Subcellular localization of aPKC proteins (red) and ZO-1 (green) in the pseudostratified retinal neuroepithelium at 32 hpf. (a) aPKCs localize to the ventricular surface of the retina. (b) aPKC proteins are slightly apical to and partially overlapping with ZO-1 at apical adherens junctions in wild-type embryos. (c) In *has* mutants, aPKCs show similar localization with respect to ZO-1, but the amount of aPKC protein is greatly reduced. **(d–f)** 60 hpf. (d) aPKCs (red) continue to localize near ZO-1 (green) at the ventricular surface of the wild-type retina. (e) ZO-1 (green) colocalizes with β-catenin (red), indicating that aPKC proteins likely localize to adherens junctions. (f) There is a profound reduction of ZO-1- and β-catenin-positive junctions at the ventricular surface in *has* mutants, indicating that most apical adherens junctions are missing by 60 hpf. **(g,h)** Alexa568-conjugated phalloidin staining (in grayscale) of the retina at 72 hpf. (g) In wild-type, a columnar epithelium of photoreceptor cells is present at the ventricular surface of the retina. (h) In *has* mutants, a disorganized layer of rounded cells is observed at the ventricular surface. With the exception of (a), the apical or ventricular side is oriented toward the top.

divisions in *has* mutant retinae display reoriented spindles, and this incidence increases to 28.1% at 50 hpf (Table 1). These observations are consistent with spindle orientation defects observed in *Drosophila aPKC* mutants and suggest that aPKCλ is required for mitotic spindle orientation during retinal progenitor cell divisions in vertebrates.

Discussion

In this report, we show that the zebrafish *has* gene encodes aPKCλ. *has* represents the first mutation identified in the highly conserved Par-3/Par-6/aPKC complex in a vertebrate organism. Previous work has suggested that localization of this complex to the tight junction is required for proper apicobasal polarity in mammalian epithelial cells [7, 8]. Here, we provide genetic evidence that aPKCλ is required for the formation and maintenance of the zonula adherens during early stages of epithelial morphogenesis. It is possible that localization to tight junctions may correspond to a later role for this protein in mature epithelia.

While our results strongly suggest that has^{m129} and has^{m567} encode kinase-inactive versions of aPKCλ, some aPKC activity is provided by aPKCζ and maternal aPKCλ in *has* mutants (see the Supplementary material). The partial functional overlap of these aPKCs helped reveal discrete aspects of aPKCλ's role in establishing epithelial polarity. Zygotic aPKCλ appears to be the only aPKC expressed within the endodermal epithelium of the swimbladder. Consequently, these cells do not form a clear epithelium in *has* mutants. In the intestine, where aPKCζ is also expressed, a polarized epithelium forms, but some aspects of zonula adherens formation are abnormal in *has* mutants. Our results show that adherens junctions cluster less efficiently during initial cell polarization and lumen formation in this organ. In *Drosophila*, Par-3 (Bazooka) directs the apical clustering of spot adherens junctions to form the zonula adherens during gastrulation [3], which suggests that this particular function of the Par-3/Par-6/aPKC complex may be conserved between flies and vertebrates. Finally, the progressive loss of apical adherens junctions in the retina and neural tube of *has* mutants demonstrates a requirement for aPKCλ in the maintenance of the zonula adherens. It is probable that maternal aPKCλ is sufficient to establish the zonula adherens in these tissues and that the junctions gradually degrade when there is no functional zygotic protein to replace maternal stores.

Within *has* mutant retinae, we also observed an increased number of reoriented spindles during progenitor cell division. Studies of mammalian cortical progenitor cells have suggested that daughter cells are generated by two types of cell divisions during neurogenesis: symmetric divisions, in which mitotic spindles orient parallel to the ventricular surface and give rise to two progenitor cells, and asymmetric divisions, in which the mitotic spindles are roughly perpendicular to the ventricular surface and may give rise to one progenitor and one differentiating cell [22]. One model for the control of spindle orientation during this process postulates that a single polarity cue aligns the mitotic spindle parallel to the ventricular surface. During asymmetric division, this polarity cue is ignored and spindle orientation is randomized, resulting in a subset of spindles with perpendicular orientation [28]. *has* mutants

Figure 6

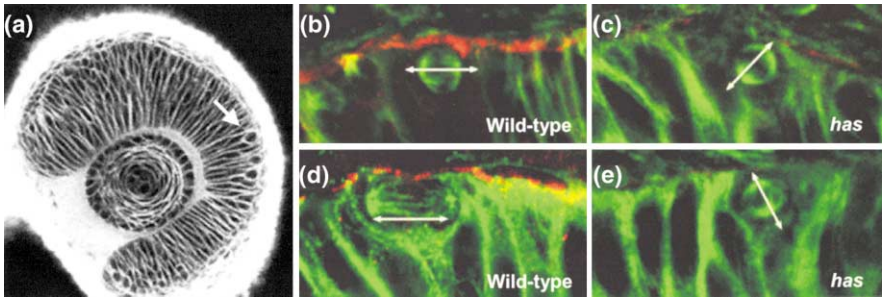

Spindle orientation defects within the *has* mutant retinal neuroepithelium. **(a–e)** The retina at 30 hpf. (a) The eye of a live *has* mutant stained with BODIPY-ceramide. The gross morphology of the retinal neuroepithelium is indistinguishable from wild-type at this stage, and most cell divisions occur at the ventricular surface (white arrow). (b) In wild-type, an antibody against α-tubulin (green) labels the mitotic spindle and reveals that most divisions are oriented parallel to the ventricular surface in metaphase (double arrows). (d) aPKC proteins (red) localize to the apical side of dividing retinal progenitor cells and appear to segregate to both daughters when the division occurs parallel to the ventricular surface. (c,e) Within the *has* mutant retina, the ratio of mitotic spindles reoriented at least 45° degrees out of the plane of the epithelium is increased, and this phenotype becomes more pronounced with time. Note the reduction of aPKC immunoreactivity in *has* mutants. Except for in (a), the apical or ventricular side is oriented toward the top.

may lack the polarity cue required to align the spindle parallel to the ventricular surface. Work from *Drosophila* has suggested that apical adherens junctions anchor the mitotic spindle within the plane of an epithelium [29]. It remains to be determined whether loss of adherens junctions leads to the reoriented spindles in *has* mutants or whether aPKCλ regulates spindle orientation through localization of proteins that serve a function similar to that of Inscuteable in *Drosophila* neuroblast divisions [6], or both.

Although there is now considerable evidence that aPKCs play a role in the formation and maintenance of polarized epithelia, no role has yet been described for aPKCs in mesenchymal tissues during development. It is interesting to speculate that loss of aPKCλ from the mesenchyme surrounding the digestive tract is responsible for the defects in gut looping and endodermal organ morphogenesis in *has* mutants. Indeed, there is extensive communication between the mesoderm and endoderm during digestive tract formation [30]. In addition, we have found that the genetic reduction of digestive tract mesoderm leads to defects in gut looping and endodermal organ morphogenesis that are extremely similar to those seen in *has* mutants (unpublished data). It will be important to determine whether aPKCλ indeed functions within the mesenchyme to control gut looping and endodermal organ morphogenesis, and if it does, whether it functions together with Par-3 and Par-6 or through some novel pathway.

Conclusions

Positional cloning of the zebrafish *has* gene reveals that it encodes aPKCλ. Our phenotypic studies of the *has* mutant indicate that aPKCλ acts at the adherens junction, as opposed to the tight junction during the initial formation of polarized epithelia. In particular, our analysis of the developing intestinal epithelium in *has* mutants indicates that aPKCλ may function in the apical targeting of ad-

Table 1

Increased incidence of spindle reorientation in *has* mutant retinae.

Age	Genotype	Number of embryos	Degree of spindle reorientation		Standard error
			0°	≥45°	
32 hpf	wt	37	141 (95.9%)	6 (4.1%)	(±1.25%)
	has	17	48 (90.6%)	5 (9.4%)	(±2.71%)
	MO	11	65 (89.0%)	8 (11.0%)	(±3.81%)
40 hpf	wt	15	53 (94.6%)	3 (5.4%)	(±2.44%)
	has	8	27 (81.8%)	6 (18.2%)	(±7.5%)
50 hpf	wt	14	49 (92.5%)	4 (7.5%)	(±2.92%)
	has	12	23 (71.9%)	9 (28.1%)	(±7.44%)

Over time, the related incidence of reoriented spindles increases in *has* mutant retinae. At 32 and 40 hpf, when apical adherens junctions in the retina still look relatively normal in *has* mutant embryos, there is a clear increase in the incidence of reoriented spindles as compared to wild-type (Figure 5 and Supplementary material). Embryos injected with *aPKCλ* MO at 32 hpf display a higher incidence of reoriented spindles than *has* mutants at the same stage, further indicating that morpholino injection appears to be more efficient at removing endogenous gene function (see the Supplementary material).

herens junctions to form the zonula adherens. Analysis of the retina and neural tube in *has* mutants shows that aPKCλ is also required for the maintenance of the zonula adherens. In addition to the various epithelial defects observed in *has* mutants, there are striking defects in endodermal organ morphogenesis. Given the expression of aPKCλ in the digestive tract mesoderm, we propose that the defects in gut looping and endodermal organ budding may be independent of the epithelial defects in the digestive tract endoderm and may represent a novel role for aPKCλ during development. Finally, we demonstrate that aPKCλ is required to properly orient the mitotic spindle during progenitor cell divisions in the retina, identifying the first genetic locus required for this process in vertebrates.

Materials and methods

Genetic mapping and positional cloning

A mapping strain was created by crossing a *has*^{m129} AB male to a wild-type WIK female. Early pressure (EP) embryos were used to initially place *has* on LG2, and subsequent linkage analysis was performed on a combination of haploid and homozygous mutant diploid embryos. PCR primers within the 3′ UTR of *elrA* were used to initiate a chromosome walk to *has* using YAC (Research Genetics) and PAC clones [31]. Sequences from the recovered ends of each genomic clone were then used to identify additional clones and to determine clone overlap. Further fine mapping with single-strand conformational polymorphisms localized the *has* gene to two overlapping PACs, 70N12 and 238M4. To identify cDNAs encoded on the 70N12 and 238M4 PACs, the inserts were excised with NotI and purified by pulsed-field gel electrophoresis. Radiolabeled probes were prepared as described [32] and used to screen a 24-hpf normalized cDNA filter (RZPD). Sequences from several partial cDNA clones and one full-length cDNA clone (ICRFp524H18162Q8) were used to assemble the full-length sequence for zebrafish *aPKCλ*. To identify the mutant lesions, cDNA was prepared from pools of 60 *has*^{m129} and *has*^{m567} mutant embryos. Three overlapping fragments from the coding sequence of *aPKCλ* were PCR amplified from both cDNA pools and cloned into the pGemT vector (Promega) for sequencing.

DNA constructs and mutagenesis

Murine aPKCλ pCMV5 Flag and kinase-inactive aPKCλ pCMV5 Flag were obtained from Christopher L. Carpenter (Division of Signal Transduction, Beth Israel Deaconess Medical Center). To engineer the *m129* and *m567* truncations, it was necessary to generate aPKCλ with an amino-terminal Flag epitope tag. To accomplish this, the carboxy-terminal Flag epitope was removed by restoring the natural stop codon using PCR mutagenesis, and the cDNA was then subcloned into pFlag CMV2 (Kodak). The R → stop mutation at position 513 (corresponding to the *m129* allele) and the W → stop mutation at position 517 (corresponding to the *m567* allele) were made using the QuikChange site-directed mutagenesis kit (Stratagene). All constructs and mutations were confirmed by sequencing.

Immunoprecipitation and Westerns

293T cells were cultured in DMEM supplemented with 10% FBS. Transient transfections were performed using Lipofectin and Opti-MEM medium (Life Technologies) as described in the manufacturer's instructions. Transfected cells were rinsed once in phosphate-buffered saline (PBS) and lysed in phospholipase C (PLC) lysis buffer with 10 μg ml^{-1} aprotonin, 10 μg ml^{-1} leupeptin, 1 mM sodium vanadate ($NaVO_3$), and 1 mM PMSF [33]. For immunoprecipitations, lysates were incubated with goat anti-mouse sepharose and with anti-Flag antibodies at a concentration of 1 μg ml^{-1} for 2 hr at 4°C. Beads were washed three times in PLC lysis buffer. Proteins were separated by SDS-PAGE, transferred to an Immobilon-P membrane (Millipore), and immunoblotted with the appropriate antibody. The antibodies that were used were the mouse monoclonal anti-Flag M2 antibody (Kodak) and the sheep polyclonal anti-phospho-PRK2 antibody, which recognizes PDK1 phosphorylation sites in a variety of enzymes, including pThr-402 of aPKCλ (Upstate Biotechnology). Blots were developed by enhanced chemiluminescence (Pierce).

Protein kinase assay

Immunoprecipitates were washed twice in PLC lysis buffer, twice in kinase reaction buffer (50 mM HEPES [pH 7.5], 25 mM $MgCl_2$, 4 mM $MnCl_2$) containing 0.1 mM $NaVO_3$, and were resuspended in 25 μl kinase reaction buffer containing 5 μCi [γ-^{32}P] ATP and 2.5 μg myelin basic protein (MBP) as a substrate. Reactions were incubated at room temperature for 30 min and were halted by the addition of 25 μl 2× SDS-PAGE sample buffer. Samples were resolved by SDS-PAGE on a 12% gel, and the incorporation of ^{32}P was detected by autoradiography.

In situ hybridization

In situ hybridizations were performed as previously described [14]. Embryos older than 24 hpf were raised in 0.003% 1-phenyl-2-thiourea (PTU, Sigma) in egg water to inhibit the production of pigment.

Antibody and phalloidin staining

For most antibody stainings, embryos were fixed for 1 hr at RT in 4% PFA in PBS. To efficiently preserve mitotic spindles, embryos were fixed in 37% formaldehyde for 25 min. After several rinses, embryos were embedded in 5% bactoagar or 4% SeaPlaque agarose (BioWhittaker Molecular Applications), and 200-μm sections were cut with a Leica VT1000S vibratome. Incubations and washes for antibody stainings were performed on floating sections in a solution of 0.1% Tween, 1% DMSO, and 5% normal goat serum in PBS. Phalloidin stainings followed a similar protocol, excluding the goat serum.

We used the following antibodies: rat polyclonal anti-PKCξ (C-20) at 1:1000 (Santa Cruz Biotechnology), mouse monoclonal anti-ZO-1 [34] at 1:25 (gift of S. Tsukita), rabbit polyclonal anti-β-catenin [35] at 1:500 (gift of P. Hausen), and mouse monoclonal anti-α-tubulin at 1:1000 (Sigma). We used secondary antibodies conjugated to rhodamine or Cy2 (Molecular Probes) at 1:400. To visualize actin, embryos were incubated in phalloidin conjugated with either rhodamine or Alexa-568 at 1:100 (Molecular Probes).

Fluorescence images were produced using either a Leica TCS NT confocal microscope or a Nikon TE 300 inverted microscope equipped with a BioRad Confocal Laser (BioRad MRC) and BioRad Laser Sharp version 3.2 software.

Live imaging

Live imaging was performed essentially as described in Cooper and D'Amico, 1999 [36]. Embryos were manually dechorionated with watchmaker's forceps in 1× Danieau's embryo medium (DEM) and placed in a vital-staining solution containing 100 μM BODIPY FL C_5-ceramide (Molecular Probes) in 1× DEM for 30 min. Subsequently, embryos were rinsed several times in DEM and embedded in 2.5% methylcellulose containing 0.1 mg/ml Tricaine (Sigma). The preparation was sealed with silicone grease to prevent evaporation. Images were recorded with the Nikon/Biorad system described above.

Accession numbers

The GenBank accession number for zebrafish aPKCλ is AF390109.

Acknowledgements

We thank David Bilder, Ira Herskowitz, Keith Mostov, Gail Martin, Nick Badovinac, and members of the Stainier lab for discussion and critical comments on the manuscript. I. Drummond, A. Tsukita, P. Hausen, and T. Kurth provided antibodies. S.H-B. is funded by a National Science Foundation Predoctoral Fellowship. S.A-S. is supported by postdoctoral fellowships of the Deutsche Forschungsgemeinschaft and the Howard Hughes Medical Institute (HHMI). T.P. is supported by an HHMI Research Scholar Award and the Medical

Research Council of Canada. Y-N.J. is an HHMI investigator. This work was funded in part by grants from the American Heart Association, the Packard Foundation, and the National Institutes of Health (HL54737) to D.Y.R.S..

References

1. Yap AS, Brieher WM, Gumbiner BM: **Molecular and functional analysis of cadherin-based adherens junctions.** *Annu Rev Cell Dev Biol* 1997, **13:**119-146.
2. Stevenson BR, Anderson JM, Bullivant S: **The epithelial tight junction: structure, function and preliminary biochemical characterization.** *Mol Cell Biochem* 1988, **83:**129-145.
3. Müller HA, Wieschaus E: ***armadillo*, *bazooka*, and *stardust* are critical for early stages in formation of the zonula adherens and maintenance of the polarized blastoderm epithelium in *Drosophila*.** *J Cell Biol* 1996, **134:**149-163.
4. Kuchinke U, Grawe F, Knust E: **Control of spindle orientation in *Drosophila* by the Par-3-related PDZ-domain protein Bazooka.** *Curr Biol* 1998, **8:**1357-1365.
5. Petronczki M, Knoblich JA: **DmPAR-6 directs epithelial polarity and asymmetric cell division of neuroblasts in *Drosophila*.** *Nat Cell Biol* 2001, **3:**43-49.
6. Wodarz A, Ramrath A, Grimm A, Knust E: ***Drosophila* atypical protein kinase C associates with Bazooka and controls polarity of epithelia and neuroblasts.** *J Cell Biol* 2000, **150:**1361-1374.
7. Izumi Y, Hirose T, Tamai Y, Hirai S, Nagashima Y, Fujimoto T, *et al.*: **An atypical PKC directly associates and colocalizes at the epithelial tight junction with ASIP, a mammalian homologue of *Caenorhabditis elegans* polarity protein PAR-3.** *J Cell Biol* 1998, **143:**95-106.
8. Suzuki A, Yamanaka T, Hirose T, Manabe N, Mizuno K, Shimizu M, *et al.*: **Atypical protein kinase C is involved in the evolutionarily conserved Par protein complex and plays a critical role in establishing epithelia-specific junctional structures.** *J Cell Biol* 2001, **152:**1183-1196.
9. Haffter P, Granato M, Brand M, Mullins MC, Hammerschmidt M, Kane DA, *et al.*: **The identification of genes with unique and essential functions in the development of the zebrafish, *Danio rerio*.** *Development* 1996, **123:**1-36.
10. Driever W, Solnica-Krezel L, Schier AF, Neuhauss SC, Malicki J, Stemple DL, *et al.*: **A genetic screen for mutations affecting embryogenesis in zebrafish.** *Development* 1996, **123:**37-46.
11. Schier AF, Neuhauss SC, Harvey M, Malicki J, Solnica-Krezel L, Stainier DY, *et al.*: **Mutations affecting the development of the embryonic zebrafish brain.** *Development* 1996, **123:**165-178.
12. Malicki J, Neuhauss SC, Schier AF, Solnica-Krezel L, Stemple DL, Stainier DY, *et al.*: **Mutations affecting development of the zebrafish retina.** *Development* 1996, **123:**263-273.
13. Stainier DY, Fouquet B, Chen JN, Warren KS, Weinstein BM, Meiler SE, *et al.*: **Mutations affecting the formation and function of the cardiovascular system in the zebrafish embryo.** *Development* 1996, **123:**285-292.
14. Yelon D, Horne SA, Stainier DY: **Restricted expression of cardiac myosin genes reveals regulated aspects of heart tube assembly in zebrafish.** *Dev Biol* 1999, **214:**23-37.
15. Johnson SL, Africa D, Horne S, Postlethwait JH: **Half-tetrad analysis in zebrafish: mapping the *ros* mutation and the centromere of linkage group I.** *Genetics* 1995, **139:**1727-1735.
16. Balendran A, Biondi RM, Cheung PC, Casamayor A, Deak M, Alessi DR: **A 3-phosphoinositide-dependent protein kinase-1 (PDK1) docking site is required for the phosphorylation of protein kinase Czeta (PKCzeta) and PKC-related kinase 2 by PDK1.** *J Biol Chem* 2000, **275:**20806-20813.
17. Belham C, Wu S, Avruch J: **Intracellular signalling: PDK1–a kinase at the hub of things.** *Curr Biol* 1999, **9:**R93-96.
18. Summerton J, Weller D: **Morpholino antisense oligomers: design, preparation, and properties.** *Antisense Nucleic Acid Drug Dev* 1997, **7:**187-195.
19. Chin AJ, Tsang M, Weinberg ES: **Heart and gut chiralities are controlled independently from initial heart position in the developing zebrafish.** *Dev Biol* 2000, **227:**403-421.
20. Nawrocki W: **Development of the neural retina in the zebrafish, *Brachydanio rerio*.** PhD Thesis, University of Oregon, Eugene, Oregon 1985.
21. Hu M, Easter SS: **Retinal neurogenesis: the formation of the initial central patch of postmitotic cells.** *Dev Biol* 1999, **207:**309-321.
22. Chenn A, McConnell SK: **Cleavage orientation and the asymmetric inheritance of Notch1 immunoreactivity in mammalian neurogenesis.** *Cell* 1995, **82:**631-641.
23. Malicki J, Driever W: ***oko meduzy* mutations affect neuronal patterning in the zebrafish retina and reveal cell-cell interactions of the retinal neuroepithelial sheet.** *Development* 1999, **126:**1235-1246.
24. Jensen AM, Walker C, Westerfield M: ***mosaic eyes*: a zebrafish gene required in pigmented epithelium for apical localization of retinal cell division and lamination.** *Development* 2001, **128:**95-105.
25. Sausedo RA, Smith JL, Schoenwolf GC: **Role of nonrandomly oriented cell division in shaping and bending of the neural plate.** *J Comp Neurol* 1997, **381:**473-488.
26. Concha ML, Adams RJ: **Oriented cell divisions and cellular morphogenesis in the zebrafish gastrula and neurula: a time-lapse analysis.** *Development* 1998, **125:**983-994.
27. Adams RJ: **Metaphase spindles rotate in the neuroepithelium of rat cerebral cortex.** *J Neurosci* 1996, **16:**7610-7618.
28. Rhyu MS, Knoblich JA: **Spindle orientation and asymmetric cell fate.** *Cell* 1995, **82:**523-526.
29. Lu B, Roegiers F, Jan LY, Jan YN: **Adherens junctions inhibit asymmetric division in the *Drosophila* epithelium.** *Nature* 2001, **409:**522-525.
30. Roberts DJ: **Molecular mechanisms of development of the gastrointestinal tract.** *Dev Dyn* 2000, **219:**109-120.
31. Amemiya CT, Zon LI: **Generation of a zebrafish P1 artificial chromosome library.** *Genomics* 1999, **58:**211-213.
32. Brownlie A, Donovan A, Pratt SJ, Paw BH, Oates AC, Brugnara C, *et al.*: **Positional cloning of the zebrafish *sauternes* gene: a model for congenital sideroblastic anaemia.** *Nat Genet* 1998, **20:**244-250.
33. Henkemeyer M, Orioli D, Henderson JT, Saxton TM, Roder J, Pawson T, *et al.*: **Nuk controls pathfinding of commissural axons in the mammalian central nervous system.** *Cell* 1996, **86:**35-46.
34. Itoh M, Yonemura S, Nagafuchi A, Tsukita S: **A 220-kD undercoat-constitutive protein: its specific localization at cadherin-based cell-cell adhesion sites.** *J Cell Biol* 1991, **115:**1449-1462.
35. Schneider S, Steinbeisser H, Warga RM, Hausen P: **Beta-catenin translocation into nuclei demarcates the dorsalizing centers in frog and fish embryos.** *Mech Dev* 1996, **57:**191-198.
36. Cooper MS, D'Amico LA, Henry CA: **Analyzing morphogenetic cell behaviors in vitally stained zebrafish embryos.** *Methods Mol Biol* 1999, **122:**185-204.